JOURNAL OF CATALYSIS **176,** 415–425 (1998)
ARTICLE NO. CA982038

FTIR Study of CO Interaction with Ru/TiO_2 Catalysts

K. Hadjiivanov,* J.-C. Lavalley,†,[1] J. Lamotte,† F. Maugé,† J. Saint-Just,‡ and M. Che‡

*Institute of General and Inorganic Chemistry, Bulgarian Academy of Sciences, Sofia 1113, Bulgaria; †Laboratoire Catalyse et Spectrochimie, CNRS UMR 6506, ISMRA—Université de Caen, 6, Bld. du Maréchal Juin, 14050 Caen Cedex, France; and ‡Laboratoire de Réactivité de Surface, URA CNRS 1106, Université P. et M. Curie, 4, Place Jussieu, 75252 Paris Cedex, France

Received December 8, 1997; revised February 4, 1998; accepted February 4, 1998

A Ru/TiO_2 (anatase) sample prepared by ion-exchange was studied by TPR and FTIR spectroscopy of CO adsorbed at different temperatures. Two kinds of Ru^{n+} species, differing in their reducibility, are present on the sample surface. The IR spectra of the sample and of CO adsorbed reveal the existence of a RuO_2-like phase and Ru^{n+} ($1 \leq n \leq 3$) cations. The supported ruthenium is completely reduced to Ru^0 after treatment with hydrogen at 523 K. Simultaneously, a large part of the initial anatase sites are liberated for exchange. Therefore, a second ion-exchange of Ru/TiO_2 is possible which allows to double ruthenium concentration. Low-temperature CO adsorption on the reduced Ru/TiO_2 catalyst reveals the existence of Ru^0 sites as well as different sites typical of the bare titania. At temperatures close to the ambient one, CO interacts with the Ru^0 clusters causing disruption of some Ru–Ru bonds and increase in dispersion of ruthenium particles. At higher temperatures, CO dissociates on particular Ru^0 sites, thus oxidizing some Ru^0 atoms to Ru^{n+} ions. Subsequently, $Ru^{n+}(CO)_3$ species are formed after adsorption of additional CO molecules on these latter species. Simultaneously, the titania sites that have been liberated during the reduction are re-occupied. On the Ru/TiO_2 catalyst whose dispersion has been modified by CO contact, further reduction with hydrogen at 523 K leads to a new drop of the metal dispersion (similar to that of freshly reduced catalyst) showing that the metal sintering/increase in dispersion are reversible effects. When CO adsorption is performed on an oxidized catalyst, both $Ru^{n+}(CO)_3$ and $Ru^{m+}(CO)_2$ species are formed on the surface. All these phenomena are also observed on the Ru/TiO_2 (anatase) catalyst prepared by impregnation. The results differ only in some quantitative values.

1. INTRODUCTION

The supported ruthenium catalysts have been widely studied during the past years. This interest is due to their good catalytic properties in many reactions. Thus, ruthenium shows a high activity and selectivity towards formation of straight-chain hydrocarbons from CO hydrogenation (1–3). It is also used for hydrogenation of aromatic compounds (4). Good catalytic properties of ruthenium are reported for hydrogenolysis (5) and homologation (6, 7) of hydrocarbons, reduction of aromatic acids (8) and aromatic nitrocompounds (3), and cis-trans isomerization of cyclohexanols (9). Promising is the use of ruthenium catalysts in the $DeNO_x$ process (3, 10).

The study of CO adsorption on supported ruthenium catalysts is important not only for the understanding of the mechanism of CO hydrogenation but also for their surface characterization. CO is one of the most used probe molecules, revealing the oxidation and the coordination state of the sites to which it is bound (11, 12). There are many works dealing with CO adsorption on supported ruthenium catalysts (13–45). The results obtained are more complicated than those observed with most other metals and the formation of different kinds of carbonyls has been proposed: Ru–CO, Ru_2CO, Ru_3CO, $Ru(CO)_2$, $Ru(CO)_3$, $Ru_2(CO)_3$, $Ru_3(CO)_{12}$, Ru^+–CO, Ru^{2+}–CO, Ru^{3+}–CO, Ru^{4+}–CO, $Ru^{\delta+}$–CO, $Ru^{2+}(CO)_2$, $Ru^{3+}(CO)_2$, $Ru^{\delta+}(CO)_3$, $Ru^+(CO)_3$, $Ru^{2+}(CO)_3$, $Ru^{3+}(CO)_3$, $Ru^{\delta+}(CO)_4$, Ru_2^-–CO, and $Ru_2^{\delta-}$–CO (see Table 1). In general, the CO bands arising from CO adsorption on supported ruthenium catalysts are divided into three groups: HF_1 (high-frequency 1) at 2156–2133 cm^{-1}, HF_2 at 2100–2060 cm^{-1} and LF (low-frequency) bands at about 2040 ± 40 cm^{-1}. Analysis of the literature data allows to distinguish at least three different kinds of species associated with the above bands:

Type I carbonyls (Ru^0–CO). The results on CO adsorption on ruthenium single crystals show, undoubtedly, that the linear metal Ru^0–CO carbonyls are characterized by a LF band at about 2040 cm^{-1} (46–48). The maximum of this band depends strongly on the coverage (24, 30, 31, 46). Thus, with the Ru/ZnO system LF is detected at 2055 cm^{-1} for $\Theta_{max.}$ and at 2000 cm^{-1} for Θ_0 (24). This band slightly decreases in intensity after evacuation at room temperature (31, 39, 49) and a complete exchange between Ru^0–^{12}CO species and ^{13}CO proceeds at room temperature (15, 36). This indicates a moderate stability of the linear metal carbonyls. It should be noted that the absorption frequency is not a sufficiently reliable criterion for identification of

[1] All correspondence should be send to J. C. Lavalley. E-mail: lavalley@ismra.fr.

0021-9517/98 $25.00

TABLE 1

Proposed Assignments of the HF_1 and HF_2 Bands Observed after CO Adsorption on Supported Ruthenium Catalysts

Species	Frequencies	Support	Comments	Ref.
$Ru^{\delta+}(CO)_4$	≈2150, ≈2100	SiO_2, Al_2O_3, HY		13
$Ru^{2+}(CO)_3$	2112, 2072	Al_2O_3	sulfided sample	14
$Ru^{2+}(CO)_3$	2148–40, 2086–75	SiO_2		15, 16
$Ru^{2+}(CO)_3$	2138, 2065	MgO		17
$Ru^{+}(CO)_3$	2055, 2005, 1960	NaY		18
$Ru^{\delta+}(CO)_3$	2152, 2091, 2086	HY	$T_{ads} = 473$ K	19
$Ru^{\delta+}(CO)_3$	2136, 2080	SiO_2		15
$Ru^{\delta+}(CO)_3$	2140, 2072	Al_2O_3		20
$Ru^{3+}(CO)_{2(3)}$	2140–10, 2085–60	ZnO		21
$Ru^{3+}(CO)_2$	2151–32, 2090–72	TiO_2		22
$Ru^{3+}(CO)_2$	2138, 2075–70	Al_2O_3		23, 24
$Ru^{3+}(CO)_2$	2146, 2088	HX		25
$Ru^{3+}(CO)_2$	2130, 2072	MgO		26
$Ru^{3+}(CO)_2$	2138–34, 2078–74	TiO_2, Al_2O_3		27
$Ru^{2+}(CO)_2$	2065, 1970	MgO		17
$Ru^{2+}(CO)_2$	2060–57, 2000–1980	ZnO		21
$Ru^{2+}(CO)_2$	2083–70, 2029–05	Al_2O_3		23, 24, 28
$Ru^{2+}(CO)_2$	2078–74, 2004–03	TiO_2, Al_2O_3		27
$Ru^{2+}(CO)_2$	2101–2080, 2038–20	TiO_2	after 473 K evacuation	22
$Ru^{2+}(CO)_2$	2083–2070, 2026–05	SiO_2		16
$[Ru^{2+}(CO)_2]_n$	2077–45, 2005–1970	SiO_2, TiO_2	$n = 1-3$	29
$Ru^{+}(CO)_2$	2150, 2088	Al_2O_3		30
$Ru^{+}(CO)_2$	2025, 2090	NaY		18
$Ru^{\delta+}(CO)_2$	2145, 2080	SiO_2		31
$Ru^{\delta+}(CO)_2$	2060, 1986	MgO	δ is probably 2	26
$Ru^{\delta+}(CO)_2$	≈2140, ≈2070	SiO_2, Al_2O_3, HY		13
$Ru^{\delta+}(CO)_2$	2070–50, 2002–1970	Al_2O_3		20
$Ru^{\delta+}(CO)_2$	2140, 2075	Al_2O_3	$\delta = 1$ or 3	32
$Ru^{\delta+}(CO)_2$	2092, 2031	HY	$T_{ads} = 473$ K	19
$Ru^{0}(CO)_2$	2146, 2085	SiO_2		33
$Ru^{2+}(CO)_x$	2156, 2100, 2086	HY		34
$Ru^{\delta+}(CO)_x$	2140–32, 2090–80	TiO_2	$x > 2$ [34]	35, 36
$Ru^{0}(CO)_x$	2148–33, 2086–70	HZSM–5		37
$Ru^{0}(CO)_x$	2030	SiO_2		38
$Ru^{0}(CO)_nX_m$	2140	SiO_2	X = O, Cl, H_2O	38
$Ru^{0}(CO)_x$	2142–40	TiO_2		35
$Ru^{0}_n(CO)_x$	2075	HY		34
Ru^{4+}–CO	2074*	SiO_2	*weak adsorption	39
Ru^{4+}–CO	2138, 2079, 2021	HY		34
Ru^{4+}–CO	2144–35	SiO_2		29
Ru^{3+}–CO	2075–70	SiO_2		29
Ru^{3+}–CO	2020, 2008	SiO_2		39
Ru^{2+}–CO	2040*, 2086–80	SiO_2	*weak adsorption	39
Ru^{2+}–CO	2034	SiO_2		29
$Ru^{2+}(NH_3)_5CO$	1950	NaY		18
Ru^{+}–CO	2146*, 2143–40	SiO_2	*weak adsorption	39
Ru^{+}–CO	2080	MgO		40
$Ru^{\delta+}$–CO	2000–1985, 1950–35	TiO_2		35
$Ru^{\delta+}$–CO	2080	SiO_2		15
$Ru^{\delta+}$–CO	2140	bulk Ru(001)	oxidized surface	41
$Ru^{\delta+}$–CO	2150–35	SiO_2		42
$Ru^{0}X_mCO$	2080	SiO_2	X = O, Cl, H_2O	38
O–Ru^{0}–CO	2080	SiO_2		42
Ru–CO	2141–37	Al_2O_3		28

Ru^0–CO carbonyls because vibrations of ionic carbonyls may also be observed in the same region (see below, type III carbonyls).

Type II carbonyls (characterized by the HF_1–HF_2 set of bands). Despite the good reproducibility in the observation of the HF bands, their interpretations are quite contradictory (see Table 1). It has been established that (i) these two bands characterize ionic carbonyls and (ii) the HF_1 and at least part of the HF_2 bands represent vibrations of $Ru^{n+}(CO)_x$ multicarbonyls (13–17, 19–27, 31, 32, 34–36). It has been found that the HF bands also appear after CO adsorption on completely reduced samples. In this case, the following peculiarities should be pointed out:

- The higher dispersion of the supported metal results in more intense bands (28, 32, 50).
- The two bands develop during the time of contact between the catalyst and CO (36).
- The bands are registered at room temperature and are not observed at low temperatures (16, 32, 51). A moderate increase in adsorption temperature (e.g., up to 473 K) results in enhanced band intensities (16, 32, 36).
- Heating under CO at higher temperatures (e.g., 673 K) leads to a decrease in intensity or disappearance of the bands (31–33).
- A certain equilibrium CO pressure is needed for the formation of the HF bands. Otherwise only the LF band is observed (16, 32).
- Both bands develop more quickly in the presence of water (40, 45).

Many authors have described the parallel intensity changes of the HF_1 and HF_2 bands (13, 24, 38, 52) (intensity ratio of ca 0.54 (15)) and thus have ascribed them to vibrations of multicarbonyls. This is supported by a series of investigations on the adsorption of ^{13}CO–^{12}CO isotopic mixtures (15, 19, 24, 25, 35, 36, 53). However, the results reported differ. Some data (9, 15, 35, 36, 53) support the formation of tricarbonyls since the gradual replacement of ^{12}CO carbonyls by ^{13}CO results in formation of four bands on the place of the HF_1 band which evidences the presence of $Ru^{n+}(CO)_3$ carbonyls with a C_{3v} symmetry. Other authors (24, 25) propose, also on the basis of isotope exchange data (where only one band has been observed between ^{13}CO–HF_1 and ^{12}CO–HF_1 after partial isotopic substitution) that the HF_1 and HF_2 bands characterize dicarbonyls. Generally, the type II carbonyl species are not decomposed during evacuation at room temperature (13, 15, 19, 21, 23, 25, 26, 28, 29, 31, 33, 34, 36, 38, 39, 52–54) and are stable up to about 200°C (23, 28, 31). These data are also confirmed by the fact that at room temperature the species producing HF bands do not exchange with ^{13}CO (13, 36).

Type III carbonyls (characterized by the HF_2–LF set of bands). Irrespective of the parallel intensity changes of the HF bands during adsorption, the HF_1/HF_2 intensity ratio decreases after desorption at elevated temperatures (15, 17, 22–24, 28). This indicates that the HF_2 band is complex and part of it (and, under certain conditions, the whole band) is due not only to type II carbonyls but also to another type of compounds (type III). Many data from the literature (16, 17, 19–24, 26, 27, 29, 53) point out that the species under consideration are $Ru^{n+}(CO)_2$ dicarbonyls (where the oxidation state of ruthenium differs from its oxidation state in the type II carbonyls). These compounds are characterized by a pair of bands at 2092–2045 (HF_2) and 2038–1970 cm^{-1} (LF). Isotopic exchanges have proved that the type III carbonyls are $Ru^{n+}(CO)_2$ compounds (24).

In addition, monocarbonyls characterized by an HF_2 band have been proposed (15, 29, 39, 40).

The mechanism of formation of $Ru^{n+}(CO)_x$ carbonyls after CO adsorption on reduced catalysts has been widely discussed. Some authors (22, 35) suggest that the effect is due to ruthenium cations still left after the reduction. However, it was demonstrated that no Ru^{n+} cations exist on supported ruthenium catalysts after reduction with hydrogen at 573 K (55, 56). Other widespread opinion is the corrosive adsorption of CO, including reaction with the surface hydroxyl groups of the support (15, 16, 32). In the case of silica supported catalysts this process follows the reaction [15]

$$Ru^0 + 2SiOH^- + 3CO = (SiO^{2-})_2Ru^{2+}(CO)_3 + H_2\uparrow \quad [1]$$

This mechanism is similar to the mechanism of formation of $Rh^+(CO)_2$ carbonyls and is supported (18) by data on the intensity drop of isolated OH groups of the support after CO adsorption. However, hydrogen-bonded hydroxyls appear on the surface at the expense of the isolated OH groups and the removal of the adsorbed CO by evacuation leads to the restoration of the original spectrum in the ν(OH) region (49, 57). Moreover, all attempts to detect hydrogen have failed (49, 57). Another explanation includes dissociation or disproportionation of CO (26, 34). In this case again there is no direct evidence in favour of such a mechanism.

The aims of the present work are: (i) to study the CO adsorption on Ru/TiO_2 catalysts at different temperatures in order to clarify some unresolved problems concerning the way of interaction of CO with the catalysts; (ii) to check the possibility to apply the recently proposed technique (58) for preparation of $Ru–TiO_2$ catalysts by double ion exchange; and (iii) to elucidate the effect of the preparation technique on the properties of anatase-supported ruthenium catalysts.

2. EXPERIMENTAL

The titania sample used for the experiments was prepared by hydrolysis of titanium tetrachloride as described earlier (59), followed by 1 h calcination in air at 723 K. The B.E.T. specific surface area of this sample was 63 $m^2\,g^{-1}$ and, according to X-ray phase analysis, it consisted of anatase.

TABLE 2

Some Characteristics of the Ru/TiO_2 Samples Studied

No.	Notation	Preparation technique	Ru wt%	Color
1	RuT-1	Ion exchange	0.55	Green
2	RuT-2	Double ion exchange	1.05	Black-green
3	RuT-3	Impregnation	0.95	Orange-red

The Ru-source was 1 wt% Ru solution (pH = 2.0) prepared from commercial $RuCl_3 \cdot nH_2O$. The ion-exchange was performed as follows: the support powder was suspended in the ruthenium-containing solution for 1 h, then the liquid phase was filtered and the solid contacted again with the original solution to ensure equilibrium with the initial values of pH and ruthenium concentration. After 1 h the precipitate was filtered, washed thoroughly with water (ca 1000 ml g^{-1}) to remove the unadsorbed and reversibly adsorbed ions, and dried in air for 1 h at 353 K. To prepare a double ion-exchanged sample according to Ref. (58), part of this sample was reduced under a hydrogen flow (20 cm^3 min^{-1}) for 1 h at 523 K and subjected to a second ion exchange as described above. Another catalyst was prepared by the conventional incipient wetness impregnation technique. Some characteristics of the samples investigated and the notation used are presented in Table 2.

The IR spectra were registered on a Nicolet-MX-1 FT-IR spectrometer with a spectral resolution of 4 cm^{-1} (512 scans). A specially designed IR cell allowed scanning the spectra at ambient or low (100 K) temperature. The cell was supplied with a gas burette permitting introduction of small amounts of adsorbates. The vacuum apparatus used ensured a residual pressure below 10^{-6} Torr (1 Torr = 133.3 $N \cdot m^{-2}$). Self supporting disks (ca 10 mg . cm^{-2} each) were prepared for the IR studies.

The temperature-programmed reduction (TPR) was carried out using 5% hydrogen in helium (20 ml min^{-1}) with a heating rate of 5 $K \cdot min^{-1}$ and in a temperature range from 293 to 773 K. The sample weight was 0.1 g.

The chemical analysis (performed by the CNRS central analytical service) of Ru was made by inductive coupling plasma (ICP).

3. RESULTS

3.1. Temperature-Programmed Reduction of the Samples

The reducibility of the supported ruthenium catalysts has been studied by TPR. The TPR profile of RuT-1 contains two main peaks with maxima at 361 and 379 K, and two weaker ones at 485 and at 616 K (Fig. 1). The RuT-3 sample exhibits a similar behavior except that no peak at 485 K is observed. Moreover, the intensity ratio between the two low-temperature peaks significantly differs; that at 361 K is more intense on the RuT-3 sample. Besides, a supplementary shoulder is detected at ca 423 K. The integral intensity of the peaks observed in the case of RuT-3 is higher than that measured for RuT-1 in agreement with the higher ruthenium concentration in the sample.

The result obtained for RuT-2 mainly differs in the low-temperature region since no peak is detected at 379 K. The total hydrogen consumption of the peaks is lower than that for RuT-3 catalyst, suggesting that a part of ruthenium introduced during the first exchange stays in the reduced state after the second one.

3.2. IR Spectroscopic Studies

3.2.1. Characterization of the Support

In order to be able to unambiguously distinguish between the species due to CO adsorbed on Ru (Ru^{n+}) sites and carbonyls formed by CO interaction with anatase, the adsorption of CO on the bare support has also been studied. Attention was paid not only to the frequency of the carbonyls formed, but also to their behavior (stability, spectral shifts) since an overlapping of bands of different origin was possible on the RuT samples.

CO adsorption at low temperature on the same titania sample as that which we have used as support in this study, has already been reported in details (60). Briefly, a series of low intense bands in the 3720–3670 cm^{-1} region, due to different surface Ti–OH hydroxyls, were detected on the activated sample. CO adsorption at 100 K (Fig. 2) leads to the formation of several CO species characterized by bands at 2206 cm^{-1} (α-Ti^{4+} sites), 2179 cm^{-1} (β-Ti^{4+} sites), 2127 cm^{-1} (^{13}CO on β-Ti^{4+} sites), 2165 cm^{-1} (γ-Ti^{4+} sites),

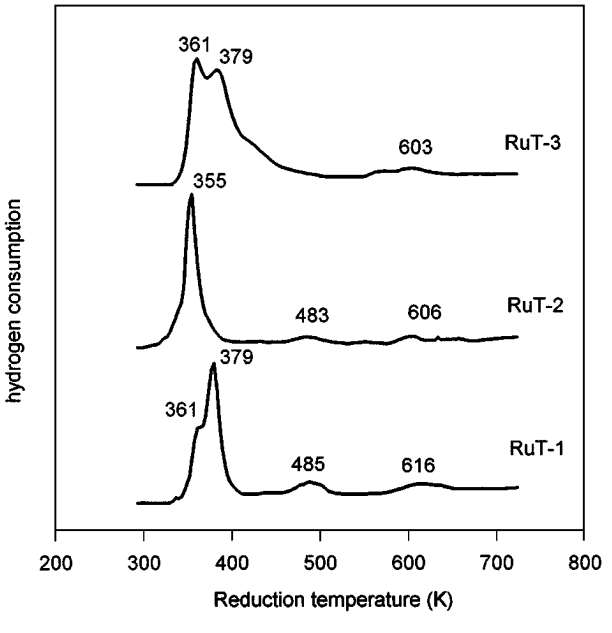

FIG. 1. TPR spectra of the samples: RuT-1, RuT-2, and RuT-3.

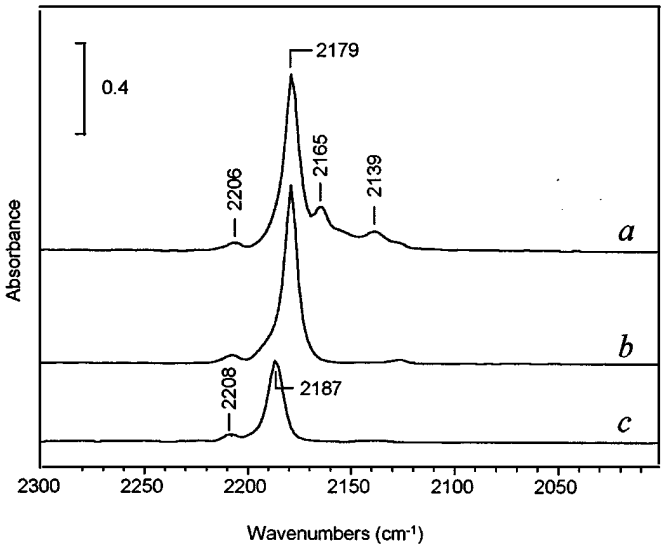

FIG. 2. IR spectra of CO adsorbed at 100 K on the anatase support. Equilibrium pressure of 1 Torr CO (a), after short evacuation until 10^{-4} Torr (b), and under dynamic vacuum of 10^{-5} Torr (c).

and 2155 cm^{-1} (OH groups) well observed under 1 Torr of CO. In addition, a band at 2139 cm^{-1}, assigned to physically adsorbed CO is also visible. After a prolonged evacuation only α and part of the β (i.e., β') Ti^{4+} sites are detected. These two bands are those observed when CO adsorption is performed at room temperature.

3.2.2. Room Temperature CO Adsorption on Oxidized and Reduced RuT-1

The RuT-1 sample has been activated by oxidative treatment (100 Torr oxygen, 1 h, 673 K) followed by 1 h evacuation at the same temperature. In the 2300–1800 cm^{-1} range, a band at 1895 cm^{-1} is observed (Fig. 3). It may be assigned to the $2\nu(Ru^{4+}{=}O)$ overtone. Many other supported oxides show overtones in this region (61). Indeed, the fundamental $Ru^{4+}{=}O$ vibration in RuO_2 supported on silica has been found at ca 900 cm^{-1} (62) which could induce an overtone band at ca 1800 cm^{-1}. This suggests that during the oxidation treatment part of the deposited Ru^{3+} has been oxidized to Ru^{4+} ions. In the ν(OH) region, the titania OH groups were detected by a band at 3670 cm^{-1} with a high frequency shoulder.

Introduction of CO to the sample thus treated leads to appearance of several bands (Figs. 3b, c). The band at 2185 cm^{-1} is the only one that changes in intensity according to the CO pressure. This is typical of CO adsorbed on the support. Three other bands at 2142, 2084, and 2036 cm^{-1} are also detected. They are not substantially affected by the CO pressure variation and by evacuation at r.t. or at 373 K (Fig. 3d). Their low wavenumbers indicate a back donation from the d level of the adsorption center to the CO antibonding $2\pi^*$ orbital. According to literature data (14–20), the bands at 2142 and 2084 cm^{-1} characterize $Ru^{n+}(CO)_3$ multicarbonyls (type II species). However, a part of the band at 2084 cm^{-1} may correspond to Ru^{n+}–CO monocarbonyl (15). The weak band at 2036 cm^{-1} well coincides in position with that characteristic for Ru^0–CO species (24, 31, 46–48). However, the presence of metal ruthenium on an oxidized sample containing also Ru^{4+} ions is not very probable. In addition, the position and behavior of the band are not typical for dispersed metal ruthenium (see below). Based on observations of other authors (19, 22–24, 28), we prefer to assign the 2036 cm^{-1} band to ionic dicarbonyls (type III species), the other ν(CO) component participating in the HF_2 band. This interpretation explains both (i) the low HF_1/HF_2 intensity ratio and (ii) the complex contour of the HF_2 band. The 2036 cm^{-1} band slightly increases in intensity after evacuation at 373 K at the expense of the $2\nu(Ru{=}O)$ band evidencing that some reduction of Ru^{4+} occurs, creating the respective Ru^{n+} sites. An important observation is that the Ti–OH groups were not affected by the CO adsorption.

The RuT-1 pellet has been reduced under hydrogen (523 K, 300 Torr H_2, 1 h) and after that evacuated at the same temperature for 1 h; the procedure was repeated three times. In such a case, no overtone of the (Ru=O) stretching vibrations is observed which confirms the above proposed assignment of the 1895 cm^{-1} band. Introduction of a small amount of CO into the cell leads to the appearance of four bands with maxima at 2144, 2110, 2083, and 2054 cm^{-1} (Fig. 4). The increase in the amount of adsorbed CO leads to (i) an increase in intensity of the bands at 2144, 2083, and 2054 cm^{-1} with a simultaneous vanishing of that at 2110 cm^{-1} and (ii) the appearance of bands due to Ti^{4+}–CO

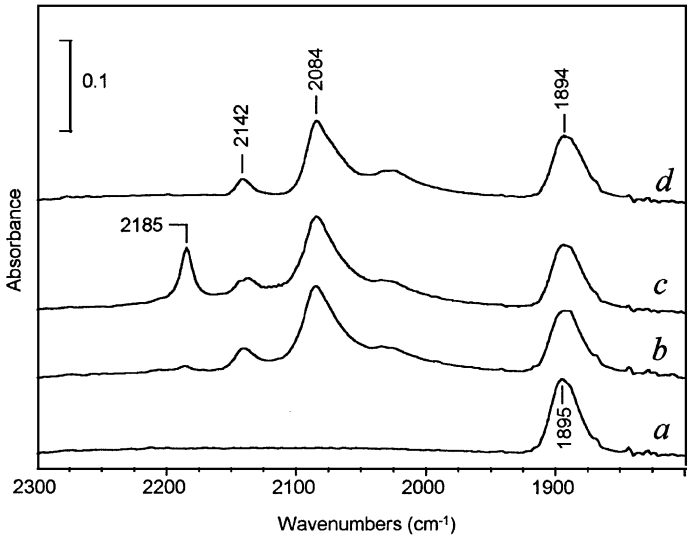

FIG. 3. IR spectra of the oxidized RuT-1 (a), after adsorption of CO at r.t. at equilibrium pressure of 1 (b) and 32 Torr (c), and after evacuation at 373 K (d).

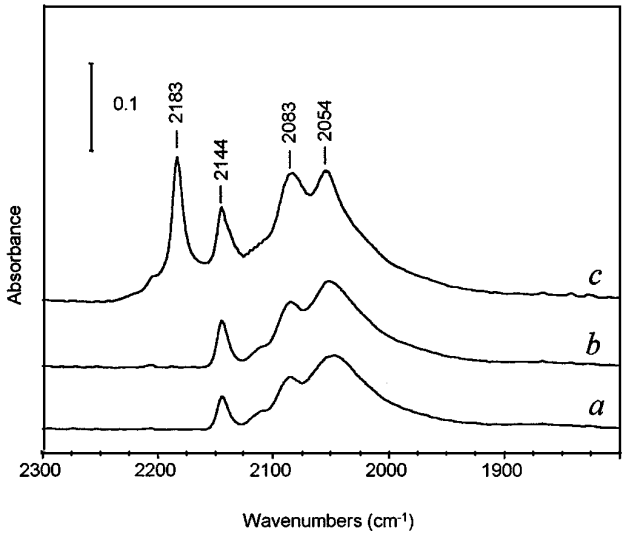

FIG. 4. IR spectra of CO adsorbed at r.t. on RuT-1 sample reduced at 523 K. Adsorption of 1 (a) and 2 (b) μmol CO and an equilibrium pressure of 32 Torr CO (c).

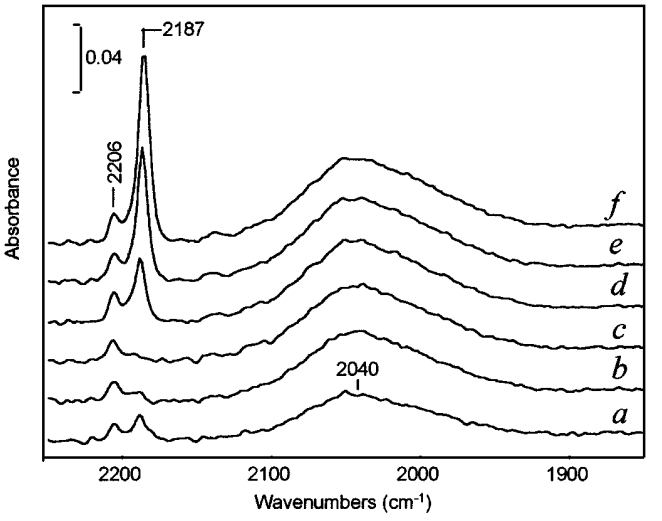

FIG. 5. IR spectra of CO adsorbed at 100 K on RuT-1 sample reduced at 523 K. Adsorption of 0.5 μmol CO (a) and the same spectrum after 2 (b) and 4 (c) min. Adsorption of 1.0 (d), 1.5 (e), and 2.0 (f) μmol CO.

complexes. However, in this case, bands for both α and β-Ti^{4+}–CO carbonyls have been observed, in contrast to the case of the oxidized sample where only β-Ti^{4+}–CO species were detected. The pair of bands at 2144 and 2083 cm^{-1} was already attributed above to $Ru^{n+}(CO)_3$ species, whereas the band at 2054 cm^{-1} is due to type I Ru^0–CO carbonyls. The band at 2110 cm^{-1}, only observed at low coverages, most probably characterizes an intermediate adsorption form, e.g., Ru^{n+}–CO. Evacuation of CO preadsorbed on reduced RuT-1 sample causes, in addition to the disappearance of the Ti^{4+}–CO bands, a shift of the LF band from 2054 to 2040 cm^{-1} and some decrease in its intensity.

3.2.3. Low-Temperature CO Adsorption on Reduced RuT-1

In order to prevent the CO induced oxidation of the ruthenium metal and to obtain more information about this process, we studied low-temperature CO adsorption on the RuT-1 sample. A pellet has been activated in the IR cell by three successive treatments, each consisting in heating 1 h at 523 K with 300 Torr H_2, followed by 1 h evacuation at the same temperature. The IR spectra of CO adsorbed on the sample at 100 K are presented in Fig. 5. Introduction of 0.5 μmol of CO into the cell leads to the appearance of a broad-tailed band with a maximum centered at ca 2040 cm^{-1} (Ru^0–CO) and two less intense bands at 2206 and 2190 cm^{-1} (Ti^{4+}–CO). With time, that at 2190 cm^{-1} tends to disappear, whereas that at 2040 cm^{-1} grows. This suggests a redistribution of the adsorbed CO from weaker Ti^{4+} support sites to stronger Ru^0 sites.

An additional increase (up to 2 μmol) of the amount of CO introduced in the IR cell leads to the re-appearance and the increase in intensity of the band at 2190 cm^{-1} which gradually shifts to 2187 cm^{-1}. The intensity of the bands at 2206 and 2040 cm^{-1} remains almost unchanged. The increase in amount of CO introduced into the IR cell up to 1 Torr (Fig. 6) leads to a shift of the band at 2187 cm^{-1} to 2177 cm^{-1} and to the appearance of some new bands, their maxima being at 2163, 2155 (shoulder), 2135, and 2124 cm^{-1}. All of these bands have already been observed on the support (60).

The gradual increase of the temperature leads to some changes in the spectrum. First of all, the intensity of the band

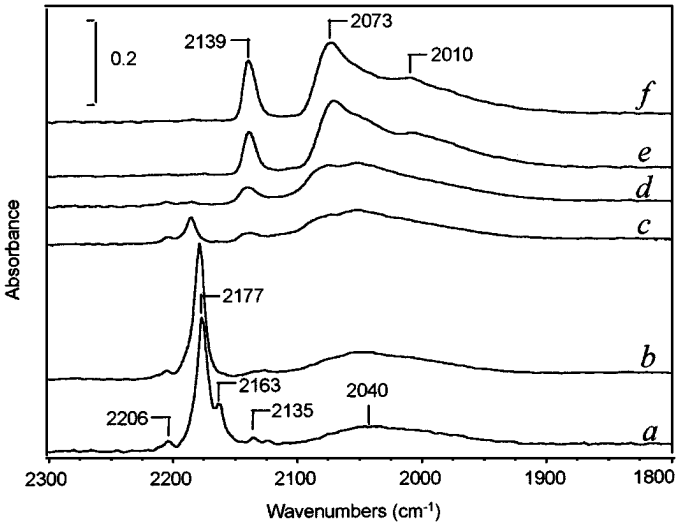

FIG. 6. IR spectra of CO adsorbed on RuT-1 sample reduced at 523 K. Adsorption of 1 Torr at 100 K (a), and time/temperature evolution of the spectra during the increase of temperature up to ambient temperature (b–d); heating the sample in CO atmosphere for 5 min at 373 K (e) and 423 K (f) (b–f spectra taken at r.t.).

at 2177 cm^{-1} decreases, whereas the 2163 and 2135 cm^{-1} bands completely disappear. Second, the band at 2040 cm^{-1} strongly increases in intensity. Moreover, bands characteristic of $Ru^{n+}(CO)_3$ species at 2139 and 2073 cm^{-1} begin to develop. These latter grow with the heating temperature up to 423 K (Figs. 6e, f). Cooling down again to 100 K in the presence of 1 Torr CO does not affect the new bands due to ionic ruthenium carbonyls. Most of the bands typical of CO adsorbed on the support reappear, except that due to α-Ti^{4+}–CO species.

The pellet thus treated has been reduced with hydrogen (1 h, 523 K) followed by 1 h evacuation at 523 K. The subsequent adsorption of CO (100 K, 1 Torr) followed by heating until 423 K leads to the same features as described above for the initially activated sample showing that the changes in dispersion and oxidation state are reversible.

3.2.4. Isotopic Exchange with ^{13}CO

On the sample heated at 473 K in CO atmosphere and then evacuated at r.t., 1 Torr of ^{13}CO has been introduced. The spectrum remains practically unchanged even after heating at 373 K (Fig. 7a). By contrast, heating at 423 K for 10 min leads to drastic changes in the spectrum (Fig. 7b). In particular, the band at 2138 cm^{-1} sharply drops in intensity, whereas new bands are noted at 2128, 2115, and 2088 cm^{-1} (with intensity increasing in the same order). In the lower frequency region, the bands overlap and thus their wavenumber cannot be exactly determined. The isotopic shift of the band at 2140 cm^{-1} coincides well with the expected shifts for ruthenium tricarbonyls which supports the assignment of this band to $Ru^{n+}(CO)_3$ species (14–20).

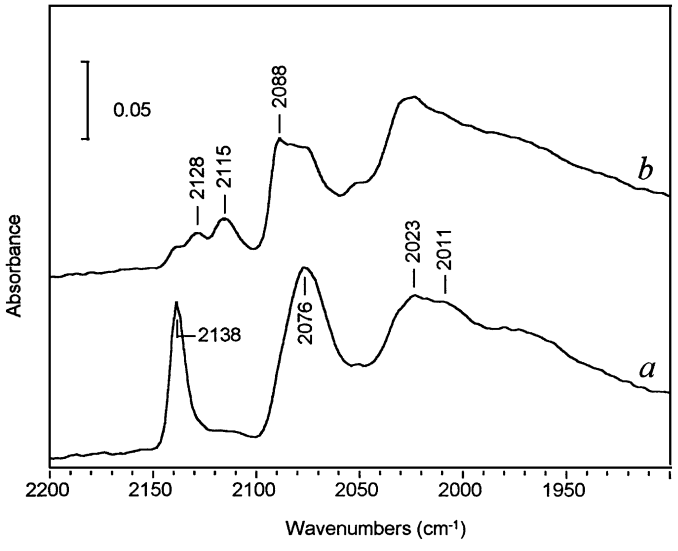

FIG. 7. IR spectra of isotopic exchange of ^{13}CO with ^{12}CO preadsorbed on RUT-1 treated as described in Fig. 6. Evacuation of the sample at r.t., introduction of 1 Torr ^{13}CO, and heating of the sample in CO atmosphere for 5 min at 373 K (a) and 423 K (b) (spectra taken at r.t.).

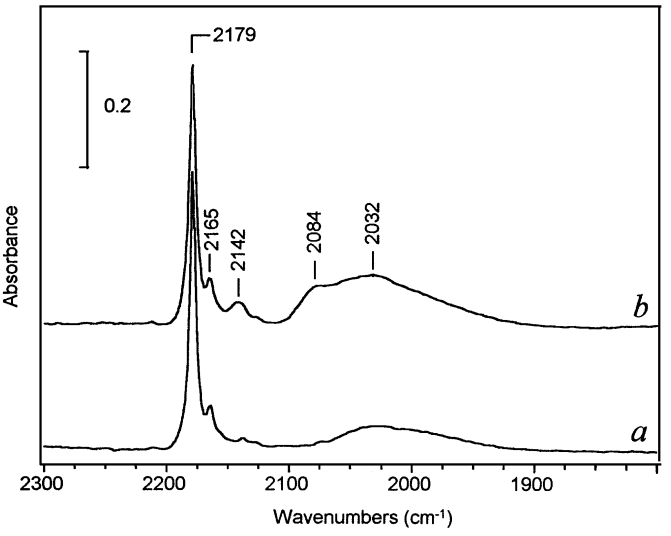

FIG. 8. IR spectra of 1 Torr CO adsorbed at 100 K on RuT-3 sample reduced at 523 K (a) and after heating the sample in CO atmosphere at 373 K for 5 min and cooling again to 100 K (b).

3.2.5. CO Adsorption on RuT-3

Some experiments have also been carried out on the reduced RuT-3 impregnated catalyst (see Fig. 8). Interestingly, the surface of the sample was almost fully dehydroxylated after the reduction/activation treatment. The low-temperature CO adsorption on the reduced sample leads again to the appearance of different species due to CO attached to the support and to Ru^0–CO carbonyls. Subsequent heating at 423 K in a CO atmosphere and cooling again to 100 K results in (i) a strong increase in intensity of the Ru^0–CO band (accompanied by its blue shift) and (ii) appearance of bands due to CO bonded to oxidized ruthenium ($Ru^{n+}(CO)_3$). As in the case of the exchange sample (RuT-1), it appears that CO has modified both the ruthenium dispersion and its oxidation degree.

4. DISCUSSION

4.1. Reducibility of the Supported Ruthenium

The TPR experiments have shown that the titania-supported ruthenium ions are easily reducible. The first two peaks observed with RuT-1 may be due either to the reduction of two different surface ruthenium species, or to a step reduction. However, we do not support the second hypothesis for two reasons: (i) the RuT-3 sample exhibits the same peaks, but with a different intensity ratio and (ii) the RuT-2 sample does not show any peak which might be assigned to the second reduction step. For these reasons, we conclude that at least two species of oxidized ruthenium, differing in their reducibility, exist on Ru^{n+}/TiO_2 samples (RuT-1 and RuT-3). The presence of metallic ruthenium in RuT-2 could explain its easier reducibility.

The peak at 483 K is observed only with the exchanged samples. We attribute this peak to hydrogen consumption due to hydrogenolysis of adsorbed organic compounds. Indeed, ruthenium is a good catalyst for hydrogenolysis at this temperature (5). Adsorption of a small amount of organic compounds during the ion-exchange procedures and especially during the washing is possible. The additional peak at 423 K observed with the impregnated catalyst may be due to another kind of ruthenium species (probably a separate phase) on the titania surface. The weak peak at about 603 K is ascribed to partial reduction of the titania surface as already observed with pure anatase (63) and Pt/TiO_2 catalysts (58) and may be associated with the appearance of the strong metal support interaction effect (SMSI).

The previous results indicate that 523 K is a temperature high enough to obtain a clean surface and to reduce all of the supported ruthenium. This latter point is confirmed by the IR spectra of low-temperature CO adsorption: no Ru^{n+} ions were detected in this case (Fig. 5). This result is in agreement with data from literature, showing that after reduction at 523 K with hydrogen, all the supported ruthenium is in the Ru^0 state (55, 56). In addition, no decoration of the metal particles with TiO_x moities is expected, since the SMSI effect is believed to occur at reduction temperatures higher than 573 K (64–66).

4.2. Interpretation of the IR Bands

The present study shows that room temperature CO adsorption on titania-supported ruthenium, whatever the sample pretreatment, results in the appearance of the HF_1 and HF_2 couple of bands, respectively at 2145–2142 and 2088–2086 cm^{-1}, characterizing oxidized ruthenium species. It is demonstrated by the experiments involving ^{13}CO (Fig. 7) that these bands characterize tricarbonyls. The corresponding monocarbonyls are probably detected only at low coverage characterized by the appearance of a small band at 2110 cm^{-1}, between HF_1 and HF_2 (Fig. 4a). The higher intensity of the HF_2 band relative to that of HF_1 in the spectra of the oxidized sample (Fig. 3) can be explained involving a supplementary band near HF_2, due to the formation of oxidized ruthenium dicarbonyls. In such a case, the other component of the ν(CO) doublet is expected at $\nu \leq 2040$ cm^{-1} (16, 22–24, 27–29). Indeed, a band at 2035 cm^{-1} band is observed on Fig. 3 (spectra b, c, and d). Therefore, it shows that the presence of this latter would not indicated the presence of Ru^0–CO species in the oxidized sample. In agreement with this interpretation, experiments involving low-temperature CO adsorption on the reduced catalyst (Fig. 5) evidence that Ru^0–CO species are characterized by a very broad band centered at 2040 cm^{-1}, shifting to 2056 cm^{-1} with coverage.

The appearance of tri- and dicarbonyls species on the oxidized sample, whereas only $Ru^{n+}(CO)_3$ species are formed on the reduced samples, suggests that the oxidation state of ruthenium is higher in the case of dicarbonyls ($Ru^{m+}(CO)_2$), i.e., m > n. Unfortunately, on the basis of our results, we are not able to specify the exact oxidation state of ruthenium in both cases.

An extra band appears near 2010 cm^{-1} after heating the reduced catalyst under CO at 373 K and more (Figs. 6e, f). We tentatively assign it to Ru^0–CO species affected by surface carbon produced by CO dissociation. However, it could also characterize ruthenium dicarbonyl species.

4.3. State and Localization of the Supported Ruthenium

The use of CO as a probe molecule allows us to determine the localization of the supported ruthenium by a close inspection of the bands typical of CO adsorption on titania. Let us recall that (i) the α sites, which present a low concentration ($\sim$0.2 sites nm^{-2}) and a high electrophility, correspond to four-coordinated Ti^{4+} cations on nonabundant planes and some edges; (ii) the β sites, correspond to five-coordinated Ti^{4+} cations and are characteristic for most of the regular faces: half of them (β' sites) adsorbs CO at r.t., the other half (β'' sites) only interacts with CO at low temperature; and (iii) the γ sites represent very weakly acidic Ti^{4+} cations situated on the (0, 0, 1) and (0, 0, $\bar{1}$) basic planes (60).

The IR spectra of CO adsorbed on the oxidized RuT-1 sample (Fig. 3) show that no α-Ti^{4+} sites are present on the surface, the concentration of the β'-sites being relatively low. We can conclude that under the conditions of the ion exchange, all of the α-sites and most probably part of the β-sites have participated to the process. These conclusions are supported by the ruthenium concentration. Thus, Ag^+, Co^{2+}, and Ni^{2+} exchanged on anatase have been found to block only the α-sites and the cation-concentration (although measured for different anatase supports) ranged between 0.2 and 0.3 Me^{n+} nm^{-2} of the anatase surface (67, 68). In contrast, Cu^{2+} ions, that have been found to block all of the α- and β'-sites, possess a surface concentration of 0.9 Cu^{2+} nm^{-2} (68). The concentration of Ru in our RuT-1 sample is 0.52 Ru^{n+} nm^{-2}, which coincides well with the proposed occupation of the α- and part of the β'-Ti^{4+} sites of anatase. This is only a small part of the support surface. For that reason, a great number of anatase sites are detected using low-temperature CO adsorption.

Discuss now what happens during the reduction of the supported ruthenium. First of all, the metal ions are reduced to Ru^0 which forms metal clusters. In addition, the reduction leads to liberation of the α and some of the β' Ti^{4+} sites as revealed by CO adsorption experiments (Fig. 5f). This is a spectral evidence of the migration of the ruthenium atoms during the reduction in order to form metal clusters.

A similar liberation of Ti^{4+} sites has been earlier observed after reduction of Pt/TiO_2 catalysts (58). In that case, the fraction of liberated sites depends on the kind of exchange. Thus, for cation exchanged samples, where Pt particles with

a mean size of about 1 nm are formed after reduction, the percentage of liberated sites (as determined by the increase in metal concentration after the second exchange) is 72%. The respective value for anion exchanged samples characterized by very small (below 0.5 nm in diameter) Pt clusters is 43%. In the case of the RuT-1 sample, the fraction of liberated sites calculated from Table 2 is 90%, which suggests formation of relatively big metal particles after reduction. This is in agreement with the appearance of bands typical of α-Ti^{4+} sites and the increase in intensity of band due to β-Ti^{4+} sites upon CO adsorption after reduction of RuT-1 sample (compare Figs. 3 and 4). On the contrary, the appearance of oxidized ruthenium sites after interaction of CO with Ru^0 is accompanied by a re-blocking of some part of the support surface. In particular, no α-sites were detected after interaction of the reduced sample with CO at 373 K.

4.4. Interaction of CO with the Ru^0 Particles

Gradual increase of temperature in the $CO-Ru^0/TiO_2$ system (Fig. 6) leads to two effects: (i) increase in intensity of the band due to Ru^0–CO species and (ii) appearance of bands typical for carbonyls of Ru^{n+} cations. This means that CO induces surface changes on the supported Ru^0 and causes an increase in its dispersion. This latter effect is more prononced for the RuT-3 sample (Fig. 8) than for RuT-1 (Fig. 6). These results show that Ru–Ru bond disruption begins to occur at temperatures lower than r.t. This disruption increases ruthenium dispersion explaining the intensity increase of the broad band at ca 2040 cm^{-1}. These results agree with some observations on Ru/Al_2O_3 and Ru/MgO catalysts describing surface changes induced by CO adsorption (49, 57). However, the same authors have not observed Ru–Ru bond breaking with Ru/TiO_2 catalysts (57). We suppose that this difference from our results might be due to the support structure (not defined in Ref. (57)) and/or to different pretreatment conditions.

The second effect observed is the appearance of $Ru^{n+}(CO)_3$ species when CO is adsorbed at room temperature (or after heating the sample in a CO atmosphere). The observation of such species is reported in most of the works dealing with CO adsorption on supported and reduced ruthenium catalysts. This phenomenon has been explained (15) for silica-supported ruthenium by corrosive CO adsorption including the surface OH groups (see Eq. [1]). However, in our cases no changes in the OH group intensity after CO adsorption was observed. Moreover, the process took place also on the almost fully dehydroxylated RuT-3 sample. This implies that after the introduction of CO in the IR cell, part of Ru^0 is oxidized directly by CO. Such a mechanism is not generally accepted, but there are many observations supporting it. Thus, ruthenium is a good Fisher–Tropsch catalyst (1–3). It is established that dissociation of the CO molecule is necessary for the formation of hydrocarbons in the $CO + H_2$ reaction (5, 65, 66). Irrespective of the fact that the reaction is usually carried out at temperatures of about 473 K, dissociation of CO on some particular ruthenium sites is possible even at the IR beam temperature. Although on the (0, 0, 1) Ru plane CO adsorption is molecular below 503 K (69), it is reported (70) that CO dissociation occurs on the steps on the (1, 1, 10) ruthenium plane at temperatures as low as 350 K. It is normal to expect that on dispersed ruthenium more defect sites and less regular planes exist. Other observations showed that only a small part of the CO adsorbed on ruthenium catalysts was desorbed after heating, whereas the main part dissociated on the surface leaving carbonaceous species (3). Unfortunately, this kind of carbon is not visible by IR spectroscopy, but there are many other proofs of its formation (65, 66). Our results suggest that there are some Ru^0 sites able to lead to CO dissociation. This phenomenon can also explain the fact that the TOF for CO hydrogenation over Ru/TiO_2 catalysts does not depend on the reduction temperature and on the kind of the support. It is believed (65, 66) that generation of TiO_x moieties on the metal surface facilitates CO dissociation, thus favouring its hydrogenation. However, such a promotion effect is necessary for supported ruthenium catalysts, since the CO dissociation over dispersed ruthenium is not hindered.

The morphology and oxidation changes occurring with supported ruthenium after its interaction with CO impeach the possibility of measuring ruthenium dispersion by CO chemisorption at room temperature. Indeed, it has been found that the measured dispersion of ruthenium is higher using CO rather than H_2 adsorption (22). This originates from both the CO-induced increase in Ru^0 dispersion and the CO consumption of the oxidation of Ru sites and formation of $Ru^{n+}(CO)_x$ species. However, correct results can be obtained by IR spectroscopy of CO adsorbed at low temperatures. On the basis of the low-temperature CO adsorption experiments, the metal dispersion on the reduced RuT-1 sample is estimated around 40%, whereas after interaction with CO at r.t. the metal dispersion increased to ~60%. Such a technique seems to be very promissing to measure metal dispersion since it avoids: (i) the CO-induced changes and (ii) the hydrogen spillover that also leads to incorrect (higher) results when H_2 is used (71).

5. CONCLUSIONS

1. The ion exchange of Ru^{3+} on anatase proceeds with the participation of the so-called α and part of the β Ti^{4+} sites and results in their blocking. RuO_2-type two-dimensional phase and other Ru^{n+} ($1 \leq n \leq 3$) species are formed on the titania surface after calcination of the catalyst.

2. Full reduction of ruthenium, deposited on anatase either by ion exchange procedures, or by impregnation, proceeds at temperatures below 523 K.

3. The reduction of the ion-exchanged samples leads to a liberation of a large part of the sites, on which the ion exchange has occurred. This allows performing a second exchange procedure and provides the possibility to increase the Ru concentration.

4. Room temperature CO adsorption on oxidized Ru/TiO_2 sample leads to the formation (in addition to the Ti^{4+}–CO species) of $Ru^{n+}(CO)_3$ and $Ru^{m+}(CO)_2$ carbonyls. On reduced samples, Ru^0–CO, $Ru^{n+}(CO)_3$, and Ru^{n+}–CO species are detected, the latter being observed only at low coverages.

5. CO adsorption at 100 K on reduced Ru/TiO_2 catalysts results in formation of Ru^0–CO species and carbonyls produced on the titania support. At elevated temperatures two other effects take place:

- increase in dispersion of the supported ruthenium induced by CO, and
- dissociation of CO molecules on particular Ru^0 sites along with formation of Ru^{n+} ions. The latter form $Ru^{n+}(CO)_3$ carbonyls.

6. The CO-induced changes are reversible; after reduction with hydrogen the initial catalyst structure is restored.

7. The use of CO adsorption at room temperature to determine the dispersion of anatase supported ruthenium leads to overestimated results (i) CO induced increase of ruthenium dispersion and (ii) CO interaction with Ru^0 resulting in formation of $Ru^{3+}(CO)_3$ species. However, low-temperature CO adsorption combined with IR spectroscopy can provide correct results.

ACKNOWLEDGMENTS

This work was supported by Gaz de France, PECO program of the European Community and the Bulgarian National Research Foundation. Thanks also to Dr. C. Louis for helpful suggestions.

REFERENCES

1. Bond, G. C., "Catalysis by Metals." Academic Press, London, 1962.
2. Biloen, P., and Sachtler, W. M. H., *Adv. Catal.* **30**, 165 (1981).
3. Zakumbaeva, G., Zakarina, N., Beketaeva, L., and Naidin, V., "Metal Catalysts." Nauka, Alma-Ata, 1982.
4. Johnson, M. M., and Nowack, G. P., *J. Catal.* **38**, 518 (1975).
5. Sinfelt, J. H., *Adv. Catal.* **23**, 91 (1973).
6. Belgued, M., Amariglio, H., Pareja, P., Amariglio, A., and Saint-Just, J., *Catal. Today* **13**, 437 (1992).
7. Rodriguez, E., Leconte, M., and Basset, J.-M., *J. Catal.* **131**, 457 (1991).
8. Smirnova, I., Tchegolya, A., and Ponomaryov, A., *J. Org. Chem.* **1**, 1402 (1965). [Russian]
9. Gurskyi, R., Litvin, E., and Freidlin, L., *in* "Catalytic Reactions in Organic Phase," p. 39. Alma-Ata, Nauka, 1974.
10. Guglielminotti, E., and Boccuzzi, F., *J. Chem. Soc. Faraday Trans.* **87**, 337 (1991).
11. Davydov, A. A., "Infrared Spectroscopy of Adsorbed Species on the Surface of Transition Metal Oxides" (C. H. Rochester, Ed.). Wiley, New York, 1990.
12. Little, L., "Infrared Spectra of Adsorbed Species." Academic Press, London/New York, 1966.
13. Qin, X., Xianxiang, S., Pinliang, Y., and Xiexian, G., *React. Kinet. Catal. Lett.* **31**, 273 (1986).
14. De Los Reyes, J. A., Vrinat, M., Breysse, M., Maugé, F., and Lavalley, J.-C., *Catal. Lett.* **13**, 213 (1992).
15. Yokomizo, G. H., Louis, C., and Bell, A. T., *J. Catal.* **120**, 1 (1989).
16. Zanderighi, G. M., Dossi, C., Ugo, R., Psaro, R., Theolier, A., Choplin, A., D'Ornelas, L., and Basset, J. M., *J. Organomet. Chem.* **296**, 127 (1985).
17. D'Ornelas, L., Theolier, A., Choplin, A., and Basset, J., *Inorg. Chem.* **27**, 1261 (1988).
18. Verdonck, J. J., Schoonheydt, R. A., and Jacobs, P. A., *J. Phys. Chem.* **87**, 683 (1983).
19. Burkhardt, I., Gudtschick, D., Landmesser, H., and Miessner, H., *in* "Zeolite Chemistry and Catalysis" (P. A. Jacobs *et al.*, Eds.), p. 215. Elsevier, Amsterdam, 1991.
20. Knözinger, H., Zhao, Y., Tesche, B., Barth, R., Epstein, R., Gates, B. C., and Scott, J. P., *Faraday Discuss. Chem. Soc.* **72**, 53 (1985).
21. Guglielminotti, E., and Boccuzzi, F., *in* "Structure and Reactivity of Surfaces" (C. Morterra, A. Zecchina, and G. Costa, Eds.), p. 473. Elsevier, Amsterdam, 1989.
22. Guglielminotti, E., and Bond, G. C., *J. Chem. Soc. Faraday Trans.* **86**, 979 (1990).
23. Beck, A., Dobos, S., and Guczi, L., *Inorg. Chem.* **27**, 3220 (1988).
24. Guglielminotti, E., Zecchina, A., Bossi, A., and Camia, M., *J. Catal.* **74**, 240 (1982).
25. Landmesser, H., and Miessner, H., *J. Phys. Chem.* **95**, 10544 (1991).
26. Guglielminotti, E., *Langmuir* **2**, 812 (1986).
27. Uchiyama, S., and Gates, B. C., *J. Catal.* **110**, 388 (1988).
28. Okuhara, T., Kimura, T., Kobayashi, K., Misono, M., and Yoneda, Y., *Bull. Chem. Soc. Jpn.* **57**, 938 (1984).
29. Evans, J., and McNulty, G. S., *J. Chem. Soc. Dalton Trans.* **80**, 1123 (1984).
30. Solymosi, F., Erdöhelyi, A., and Kocsis, M., *J. Chem. Soc. Faraday Trans. 1* **77**, 1003 (1981).
31. Davydov, A. A., and Bell, A. T., *J. Catal.* **49**, 332 (1977).
32. Solymosi, F., and Rasko, J., *J. Catal.* **15**, 107 (1989).
33. Yamasaki, H., Kobori, Y., Naito, S., Onishi, T., and Tamaru, K., *J. Chem. Soc. Faraday Trans. 1* **77**, 2913 (1981).
34. Goodwin, J. G., Jr., and Naccache, C., *J. Catal.* **64**, 482 (1980).
35. Gupta, N. M., Kamble, V. S., Iyer, R. M., Ravindranathan Thampi, K., and Grätzel, M., *J. Catal.* **137**, 473 (1992).
36. Robbins, J. L., *J. Catal.* **115**, 120 (1989).
37. Shen, J. Y., Sayari, A., and Kaliaguine, S., *Appl. Spectrosc.* **46**, 1279 (1992).
38. Chen, H. W., Zhong, Z., and White, J. M., *J. Catal.* **90**, 119 (1984).
39. Abhivantanaporn, P., and Gardner, R. A., *J. Catal.* **27**, 56 (1972).
40. Schwank, J., Parravano, G., and Gruber, H. L., *J. Catal.* **61**, 19 (1980).
41. Peden, C. H. F., and Hoffmann, F. M., *Catal. Lett.* **10**, 91 (1991).
42. Brown, M. F., and Gonzalez, R. D., *J. Phys. Chem.* **80**, 1731 (1976).
43. Kohler, J. U., and Krauss, H. L., *J. Mol. Catal.* **A123**, 49 (1997).
44. Gupta, N., Londhe, V., and Kamble, V., *J. Catal.* **169**, 423 (1997).
45. Crisafulli, C., Scire, S., Minico, S., Maggiore, R., and Galvagno, S., *Appl. Surf. Sci.* **99**, 401 (1996).
46. Kostov, K., Rauscher, H., and Menzel, D., *Surf. Sci.* **278**, 62 (1992).
47. Hoffmann, F. M., and Weisel, M. D., *Surf. Sci.* **269/270**, 495 (1992).
48. Kevin Kuhn, W., He, J. W., and Goodman, D. W., *J. Vac. Sci. Technol.* **101**, 2477 (1992).
49. Mizushima, T., Tihji, K., Udagawa, Y., and Ueno, A., *J. Phys. Chem.* **94**, 4980 (1990).
50. Dalla Betta, R. A., *J. Phys. Chem.* **79**, 2519 (1975).
51. Hadjiivanov, K., and Klissurski, D., *Chem. Soc. Rev.* **25**, 61 (1996).
52. Lynds, L., *Spectrochim. Acta.* **20**, 1369 (1964).
53. Landmesser, H., and Miessner, H., *J. Phys. Chem.* **95**, 10544 (1991).
54. Kiss, J. T., and Gonzalez, R. D., *J. Phys. Chem.* **88**, 892 (1984).

55. Bossi, A., Garbassi, F., Orlandi, A., Petrini, G., and Zanderighi, L., *Stud. Surf. Sci. Catal.* **3**, 405 (1978).
56. Blanchard, G., Charcosset, H., Chenebauz, M., and Primet, M., *Stud. Surf. Sci. Catal.* **3**, 197 (1978).
57. Mizushima, T., Tohji, K., Udagawa, Y., and Ueno, A., *J. Am. Chem. Soc.* **112**, 7887 (1990).
58. Hadjiivanov, K., Saint-Just, J., Che, M., Tatibouet, J., Lamotte, J., and Lavalley, J. C., *J. Chem. Soc. Faraday Trans.* **90**, 2277 (1994).
59. Hadjiivanov, K., Klissurski, D., and Davydov, A., *J. Catal.* **116**, 498 (1989).
60. Hadjiivanov, K., Lamotte, J., and Lavalley, J. C., *Langmuir* **13**, 3374 (1997).
61. Busca, G., and Lavalley, J. C., *Spectrochim. Acta* **A42**, 443 (1986).
62. Lopez, T., Bosch, P., Asomoza, M., and Gomez, R., *J. Catal.* **133**, 247 (1992).
63. Hadjiivanov, K., Lamotte, J., Saur, O., and Lavalley, J. C., *Z. Phys. Chem.* **187**, 281 (1994).
64. Tauster, S. Y., Fung, S. C., and Garten, R. L., *J. Am. Chem. Soc.* **100**, 170 (1978).
65. Desasco, R., and Haller, G., *Adv. Catal.* **36**, 173 (1989).
66. Vannice, M. A., *Catal. Today* **12**, 255 (1992).
67. Hadjiivanov, K., Vassileva, E., Kantcheva, M., and Klissurski, D., *Mater. Chem. Phys.* **28**, 367 (1991).
68. Hadjiivanov, K., Klissurski, D., Kantcheva, M., and Davydov, A., *J. Chem. Soc. Faraday Trans.* **87**, 175 (1991).
69. Lauderback, L., and Deglas, W., *J. Catal.* **195**, 55 (1982).
70. Shincho, E., Egawa, C., Naito, S., and Tamura, K., *Surf. Sci.* **149**, 1 (1980).
71. Komaya, T., Bell, A. T., Weng-Sien, Z., Gronsky, R., Engelke, F., King, T. S., and Pruski, M., *J. Catal.* **149**, 142 (1994).